Predictive Model Control of a Three-Phase Converter

Ramanantsihoarana Harisoa Nathalie¹; Rastefano Elisée²

^{1;2}École Doctorale Sciences Et Techniques De l'Ingénierie Et De l'Innovation EDSTII, EAD SDE Antananarivo, Madagascar

Publication Date: 2025/09/30

Abstract: This work introduces a detailed framework for a three-phase multilevel converter that incorporates model predictive control (MPC) to improve power conversion efficiency. The developed MPC approach utilizes a comprehensive cost function designed to achieve multiple objectives: accurate current control, reduction of circulating currents, and maintaining balanced capacitor voltages—all without requiring traditional modulation components. Testing performed using MATLAB/Simulink validates the system's capabilities, confirming the production of six distinct voltage levels, proper capacitor voltage regulation within design specifications. The control methodology demonstrates reliable operation during varying operating conditions, particularly when subjected to abrupt DC voltage changes that replicate practical scenarios like fluctuating solar panel output conditions.

Keywords: Average Value Model, Power Electronics, Voltage Balancing, Three-Phase Systems, Switching Frequency Optimization.

How to Cite: Ramanantsihoarana Harisoa Nathalie; Rastefano Elisée (2025) Predictive Model Control of a Three-Phase Converter. *International Journal of Innovative Science and Research Technology*, 10(9), 2131-2138. https://doi.org/10.38124/ijisrt/25sep1045

I. INTRODUCTION

Due to their dual nature, power converter control systems have conventionally been divided into two separate elements. One component focuses on the continuous aspects that govern the converter's primary interface functions, while the other handles the discrete on-off behavior of individual switches using modulation strategies. In this context, growing requirements for improved efficiency, dependability, adaptability, and overall performance demand substantial progress in the sophistication of the complete control system.

To meet these challenges, we introduce an integrated methodology that addresses both the interface requirements of power converters and their switching characteristics through a single control structure. This strategy requires the direct inclusion of power converter nonlinear behaviors within the control algorithm, thus removing the need for traditional modulation components. Modulation has historically functioned as the standard method for linearizing converter internal dynamics. The Model Predictive Control (MPC) technique has been chosen to handle this nonlinear complexity while accommodating the various control goals typical of power converters.

From this viewpoint, we develop a comprehensive control approach that simultaneously manages both the operational interface functions of converters and their switch-mode characteristics using a unified controller design. This method involves directly embedding converter nonlinear properties into the control algorithm, consequently eliminating the dependency on conventional modulation systems. Model Predictive Control (MPC) serves as the selected approach for addressing this nonlinear complexity while allowing concurrent consideration of the multiple control objectives common to power converters.

The organization of this paper follows these primary sections: the literature review examines current advances and notable research contributions in this area, the modeling portion establishes the mathematical and theoretical framework for predictive control, and the simulation analysis offers computational verification of the proposed models.

II. STATE OF THE ART

➤ Multilevel Converter

Multilevel Converters (MC) were initially developed to meet AC-AC conversion needs in electric motor drive systems [1]. These devices are built using interconnected switching modules in a cascaded arrangement, from which they derive their operational characteristics. Research focuses on two main design aspects: the overall structural layout and the choice of individual modules [2]. Based on these design decisions, different features can be optimized or minimized

by creating converters suited for particular uses. The expandable design of MC allows for easy scaling to accommodate higher voltage requirements, leading to their widespread implementation across diverse industrial sectors. A notable benefit of this configuration is its ability to perform direct AC-AC or DC-DC power conversion, thus removing the need for separate rectification and inversion components [3].

The MC structure is arranged as shown in Fig. 1. Each phase of the three-phase electrical system connects to the midpoint of its respective converter branch (*a*, *b*, *c*). Every branch contains two sections: a top section and a bottom section. Each section is made up of series-connected modules (SMs) paired with an inductor (*L*). The DC portion of the MMC, known as the DC bus, has both positive and negative connection points. The section linking the positive DC terminal to the midpoint of each converter branch is called the top section (*u*). Likewise, the section connecting the negative DC bus terminal to the midpoint of each converter branch is referred to as the bottom section (*l*).

The MC design provides numerous unique benefits that have made it the favored choice for high-power industrial applications. Its natural scalability permits easy expansion to accommodate greater voltage and power demands by incorporating additional modules, while its versatile direct AC-AC and DC-DC conversion abilities remove the necessity for intermediate processing stages. The modular construction approach allows for standardized module production, leading to economical manufacturing and servicing processes. Additionally, MC exhibits better harmonic characteristics than traditional two-level converters and offer built-in fault resistance through module bypass functions. These collective features have established MC as the preferred technology for applications such as renewable energy systems integration, and industrial motor control applications.

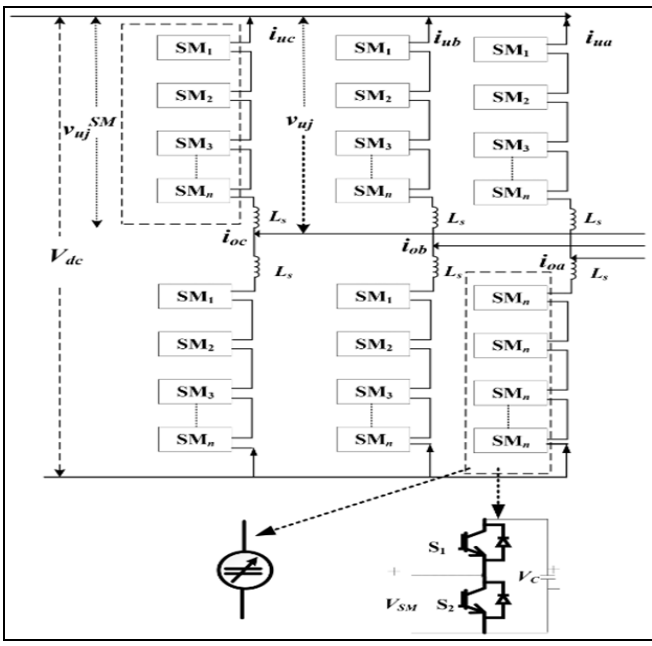


Fig 1 MC Architecture

➤ Model Predictive Control (MPC)

The control systems used in power converter operations offer significant potential for deploying sophisticated algorithmic solutions. These control methods possess adequate complexity to manage aspects of the natural nonlinear behavior while simplifying the coordination of various goals and specifications that are constantly present in power converter applications. Within these algorithmic categories, sliding mode control (SMC) and model predictive control (MPC) stand out as two leading techniques that have been effectively applied in power converter control systems.

MPC represents an optimization-driven algorithm that concurrently establishes a function for execution. This essential component, known as the cost function, is formulated to capture the system's control goals. The algorithm utilizes an internal system model to conduct closed-loop optimization through predictive analysis. For linear applications, MPC functions equivalently to a closedloop linear quadratic regulator (LQR) [4]. The general framework of MPC is depicted in Fig. 2. A key strength of MPC stems from its fundamental design: while it is commonly implemented using linear optimization techniques, both the prediction model and optimization process can be adapted for various operating conditions. Another major benefit of MPC is its capability to manage multiple-input multiple-output (MIMO) systems alongside built-in operational limits [5]. This feature proves especially valuable in power converter applications, where control demands are typically demanding and MIMO situations are common.

In modulation-based control frameworks, two MPC variants are utilized: generalized predictive control (GPC), which applies the standard linear quadratic MPC approach [6], and explicit MPC (EMPC), which uses offline parametric optimization to minimize computational requirements during real-time operation [7]. Due to its MPC optimization foundation, demands higher computational resources than traditional control approaches. However, despite this computational requirement, the approach allows for handling intricate system descriptions and operational constraints.

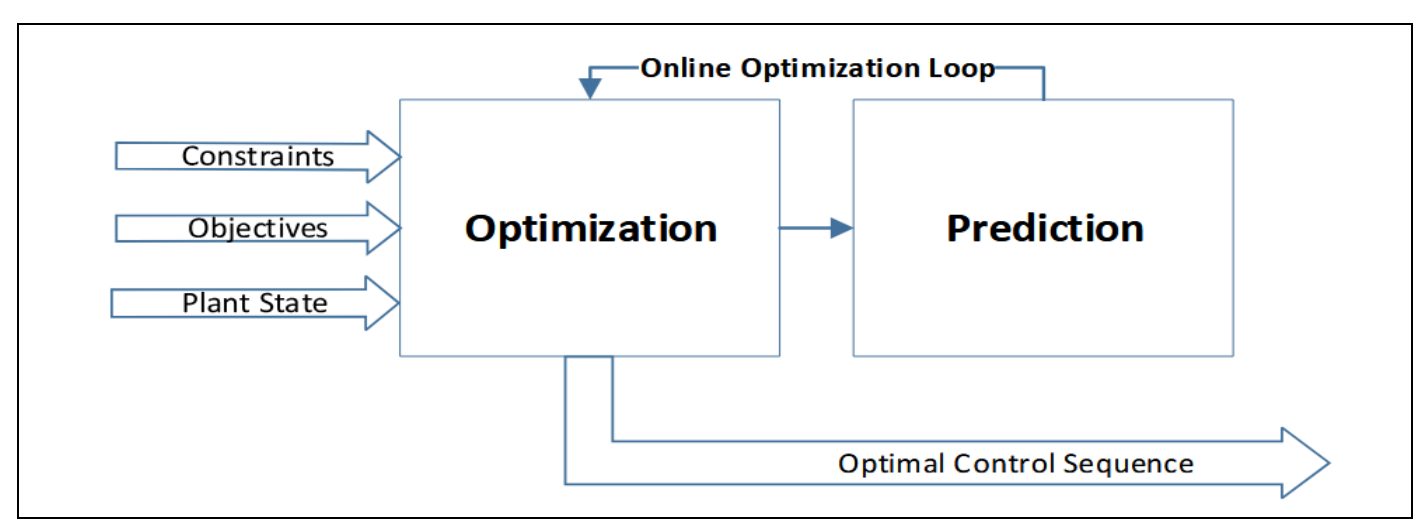


Fig 2 MPC Structure

III. METHODOLOGY

➤ Average Model of MC

The high computational demands of detailed converter models require the use of simplified Average Value Models (AVM) that can accurately capture the typical behavior of power converters and their control systems through controlled sources and streamlined mathematical functions.

In this modeling approach, modulation signals—enhanced with appropriate DC bias components—are derived from the converter's internal current control loops as shown in Fig. 3. These modulation signals then drive two equivalent controlled voltage sources that represent the upper and lower switching branchs of the MC, as depicted in the AC-side schematic of the AVM shown in Fig. 4.

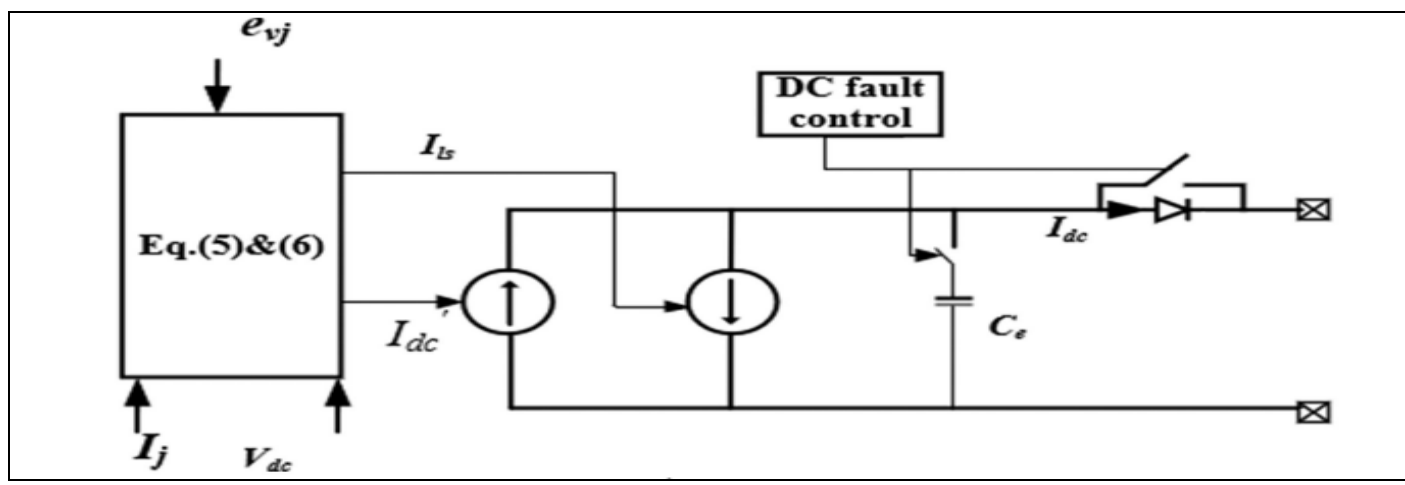


Fig 3 DC Side of the AVM

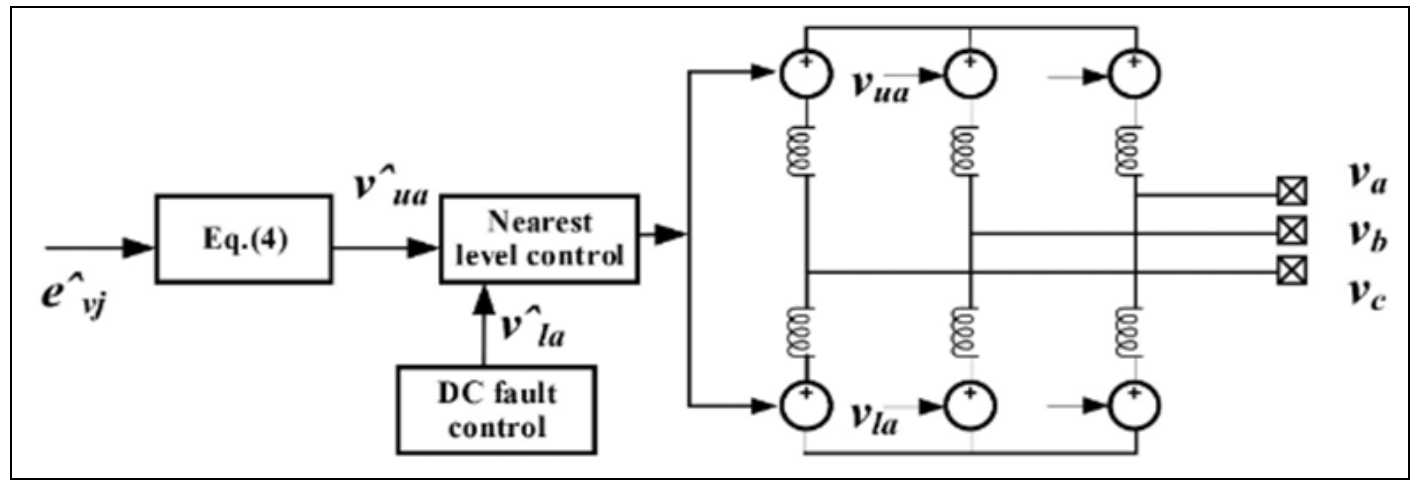


Fig 4 AC Side of the AVM

From Fig.1 we have

$$v_{u_j}^{SM} = \frac{v_{dc}}{2} - L_{arm} \frac{d_{i_{u_j}}}{dt} - v_j \tag{1}$$

And for the upper branch:

$$v_{l_j}^{SM} = \frac{v_{dc}}{2} - L_{arm} \frac{d_{i_l}}{dt} - v_j \tag{2}$$

$$i_{u_j} = \frac{i_{dc}}{3} - \frac{i_{o_j}}{2}, i_{l_j} = \frac{i_{dc}}{3} + \frac{i_{o_j}}{2}$$
 (3)

Combining (1) and (2), we have:

$$v_{u_j}^{SM} = \frac{V_{dc}}{2} + e_{v_j}, \ v_{l_i}^{SM} = \frac{V_{dc}}{2} - e_{v_j}$$
 (4)

Where

$$e_{v_j} = \frac{v_{u_j} - v_{l_j}}{2} \tag{5}$$

International Journal of Innovative Science and Research Technology https://doi.org/10.38124/ijisrt/25sep1045

This system utilizes the nearest level modulation technique. The DC-side representation of the converter, illustrated in Fig.3, is founded on the basic principle of power balance - demanding that the power on the AC side equals the power on the DC side. The mathematical foundation for modeling DC-side behavior is developed using equations (6) through (8).

$$I_{l_S} = \frac{P_{l_S}}{V_{d_C}} = R_{l_S} \frac{(l'_{d_C})^2}{V_{d_C}} \tag{6}$$

$$I'_{dc} = \frac{\sum_{j=a,b,c} (e_{v_j} * i_j)}{v_{dc}}$$
 (7)

$$I_{dc} = I'_{dc} - I_{ls} \tag{8}$$

> Cost Function of the MPC

MPC utilizes a cost function to establish the desired system behavior, where the optimal control strategy is identified by minimizing this cost function [8]. The configuration of the MPC system framework is shown in Fig. 5.

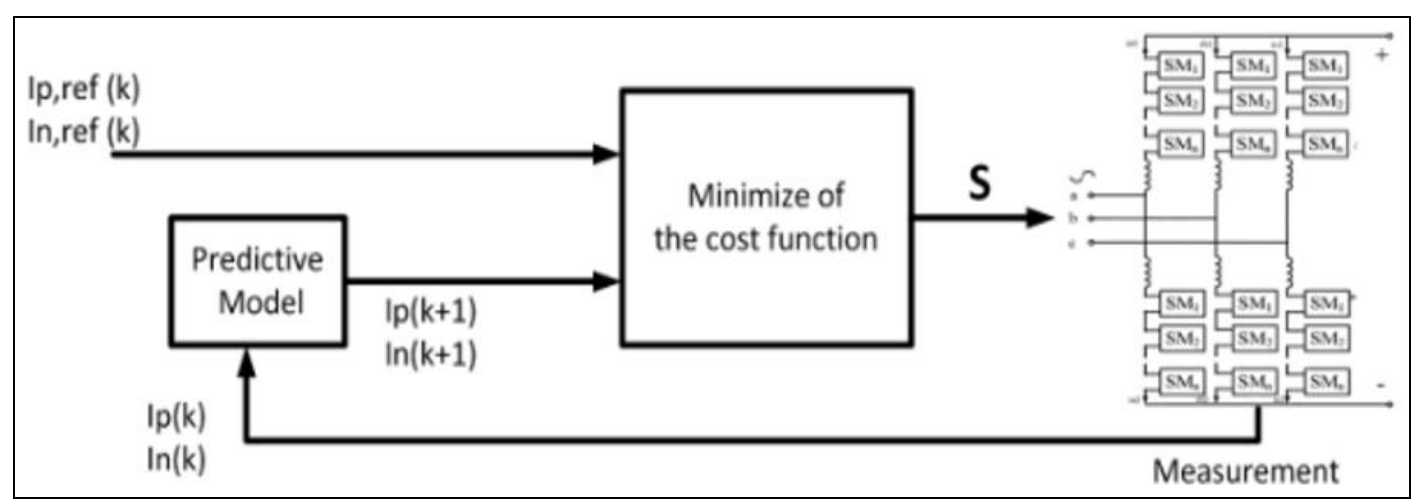


Fig 5 MPC System

The cost function formulation is based on the target system performance requirements. In this case, equation 9 defines the cost function under consideration.

In this expression, *ip,ref* and *in,ref* represent the desired reference current values, *ip* and *in* denote the forecasted current outputs, while *ip,diff* and *in,diff* correspond to the circulating currents for positive and negative sequences respectively.

$$\begin{bmatrix} J_{p}(\mathbf{k}) \\ J_{n}(\mathbf{k}) \end{bmatrix} = \begin{bmatrix} i_{p}(\mathbf{k}+1) \\ i_{n}(\mathbf{k}+1) \end{bmatrix} - \begin{bmatrix} i_{p,ref}(\mathbf{k}+1) \\ i_{n,ref}(\mathbf{k}+1) \end{bmatrix} + \lambda_{cir} \begin{bmatrix} i_{p,diff}(\mathbf{k}+1) \\ i_{n,diff}(\mathbf{k}+1) \end{bmatrix}$$
(9)

> Algorithm MPC

The controller's objective is cost function minimization, accomplished through comprehensive evaluation of all feasible switching configurations to identify the option yielding the lowest cost function value. Given that each cost function component represents the deviation between predicted and reference values, the MPC approach selects the switching configuration that produces minimal cost function results. With n submodules (SM) consistently active and n submodules inactive per phase, the complete set of switching combinations totals C_{2n}^n . Fig. 6 illustrates the flowchart of the MPC algorithm implementation.

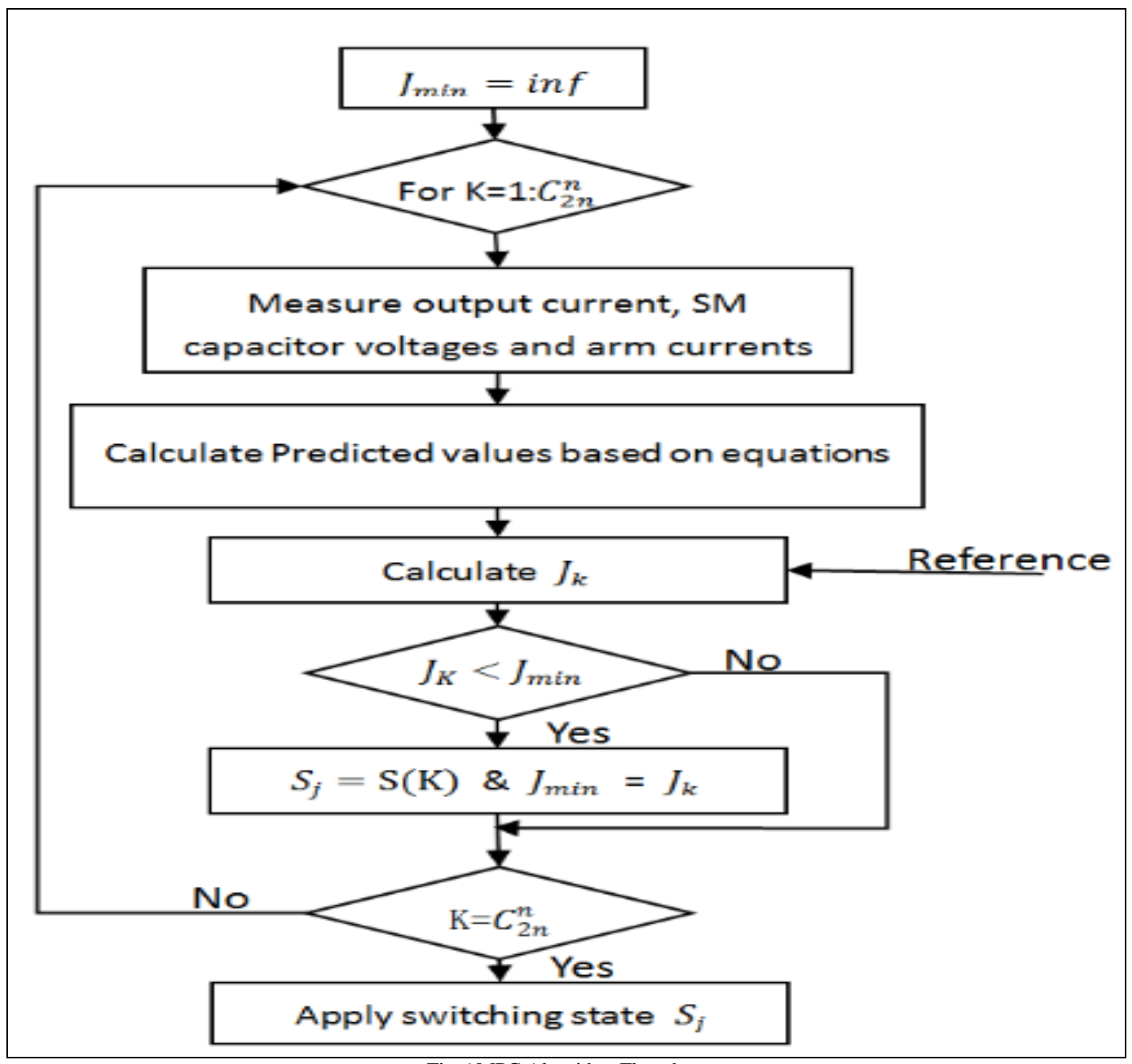


Fig 6 MPC Algorithm Flowchart

IV. SIMULATION AND RESULTS

A. Specifications of the Converter

To evaluate the performance of the model predictive control method, simulation studies are performed using the MATLAB/Simulink environment with the fundamental system specifications listed in Table 1.

Table 1 Specifications of the Converter

| Table 1 Specifications of the Converter | |
|--|-------------------------|
| Parameters | Value |
| Number of cells per branch | 6 |
| Rated frequency | 60Hz |
| Carrier frequency | 600Hz |
| Series-connected modules capacitor initial voltage | 5800V |
| Rated voltage | 10kV |
| Branch inductance | 1.59mH |
| Branch resistance | $0.04 \mathrm{m}\Omega$ |
| Cell capacitance | 100μF |

Fig. 7 presents the circuit diagram of the system simulated with Matlab.

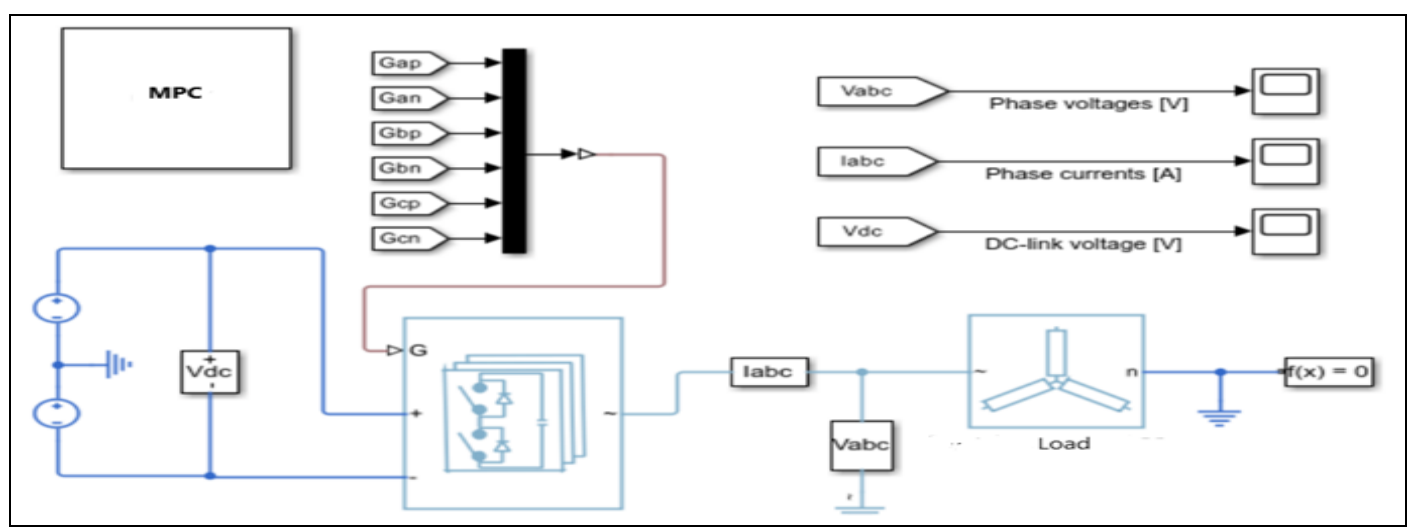


Fig 7 Circuit Diagram of the System MC-MPC

B. Results and Discussions

Fig. 8 shows the voltage waveform across the six capacitors during phase a. Charging and discharging the

capacitors causes the voltage levels to vary within acceptable limits.

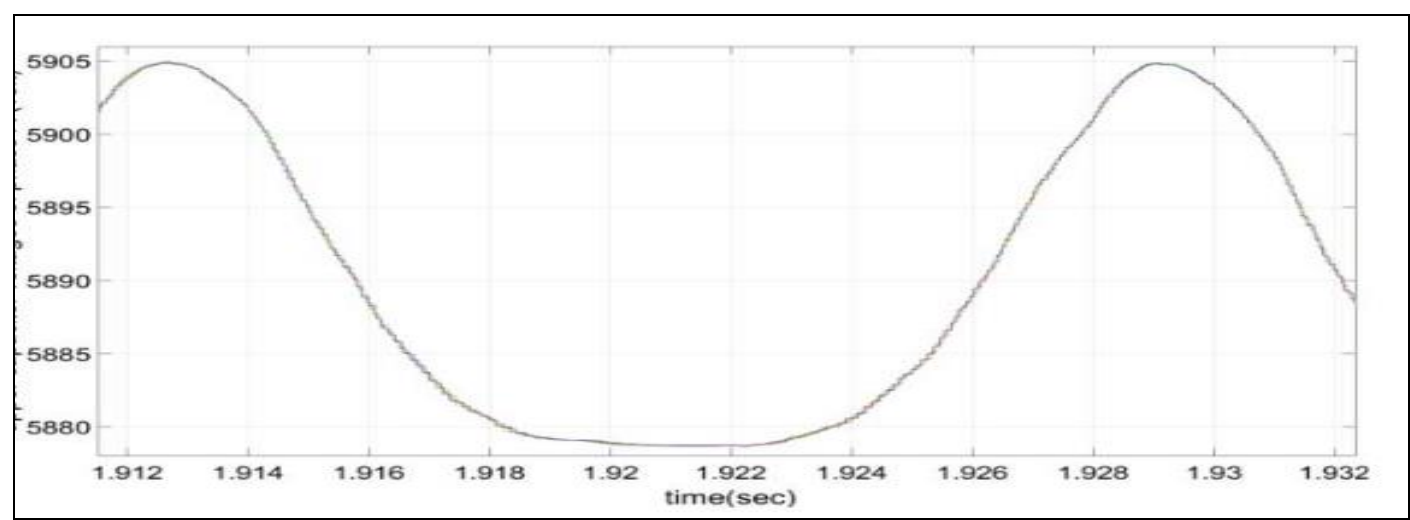


Fig 8 Voltage Waveform Across the Six Capacitors

Fig. 9 shows the three-phase voltage line by line. It clearly reveals the presence of six voltage levels.

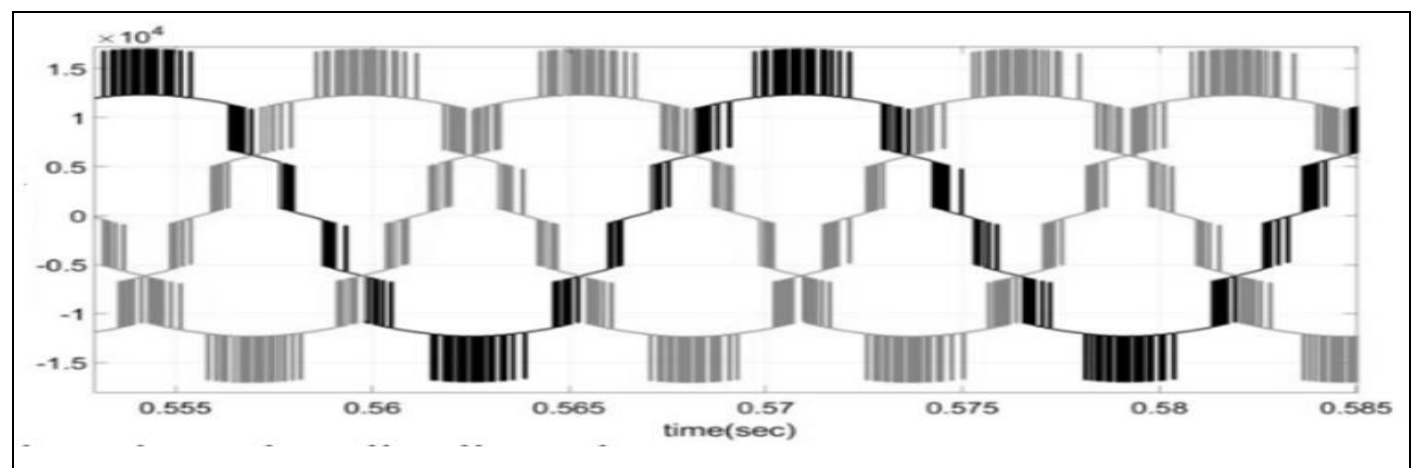


Fig 9 Three Phase Voltage

Fig.10 displays the voltage measurement across the top module of phase a. The results indicate that this module operates with 10 switching events per electrical cycle. This

produces an IGBT switching frequency of around 600 Hz, which is suitable for this power rating.

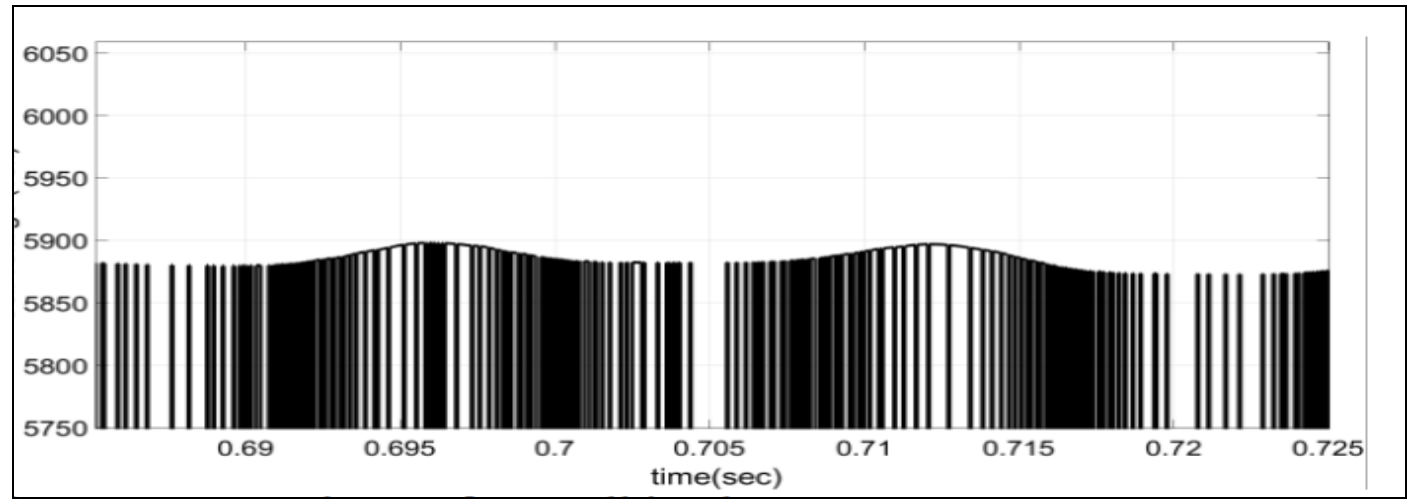


Fig 10 Voltage Across the Upper Cell

Fig. 11 shows the DC current flowing through the branchs and the DC bus. This DC current helps maintain the power balance in the capacitors.

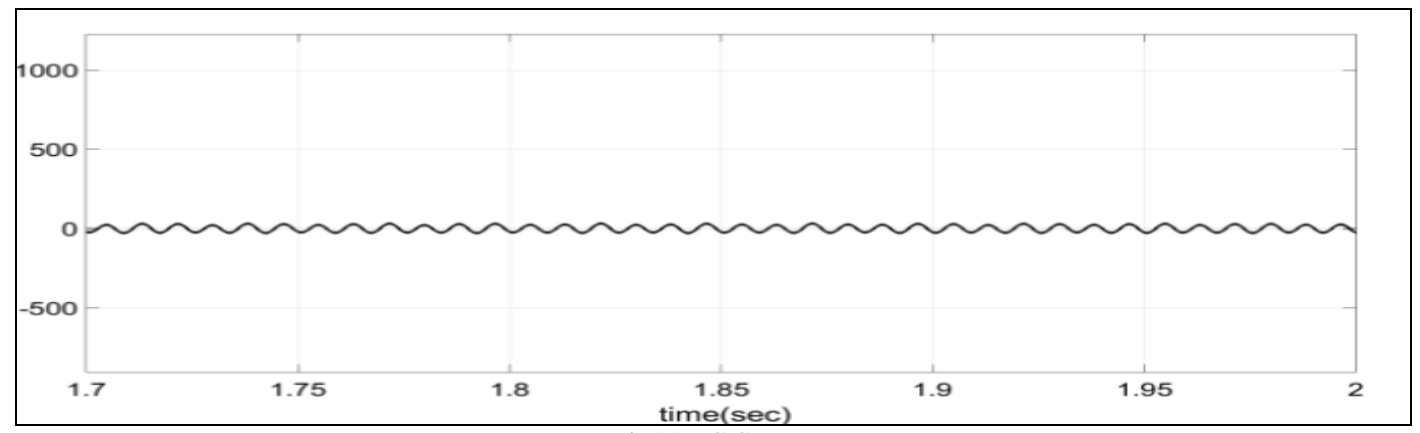


Fig 11 DC Current

To test how the developed MPC performs during fault scenarios, an abrupt change in DC bus voltage was simulated to replicate varying solar panel conditions. The MC phase currents under these circumstances are presented

in Fig. 12. Furthermore, Fig. 13 displays the branch's current behavior. The graph demonstrates that the branch current rises considerably when responding to the rapid DC bus voltage fluctuation.

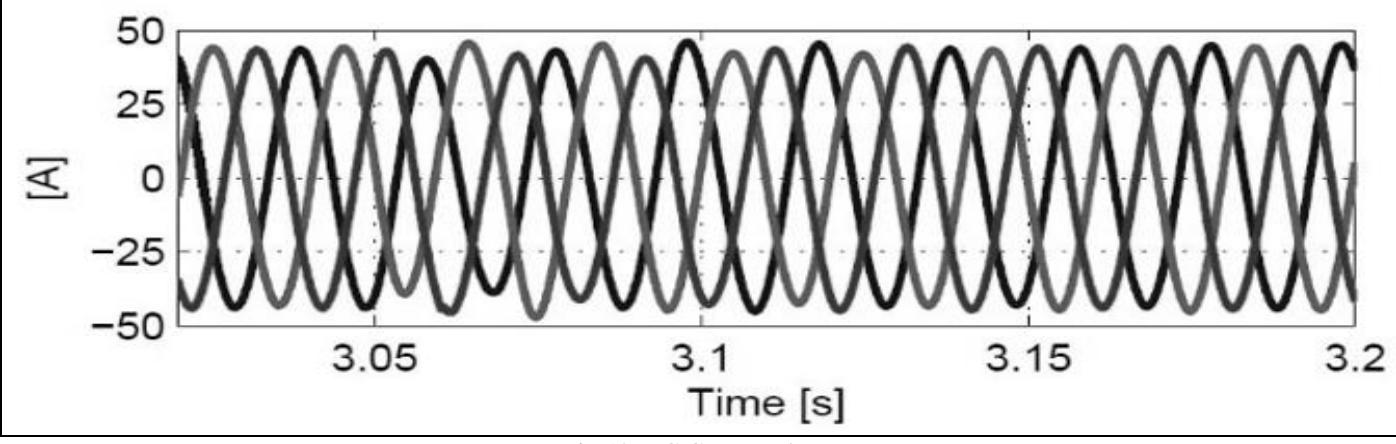


Fig 12 MC Current Phase

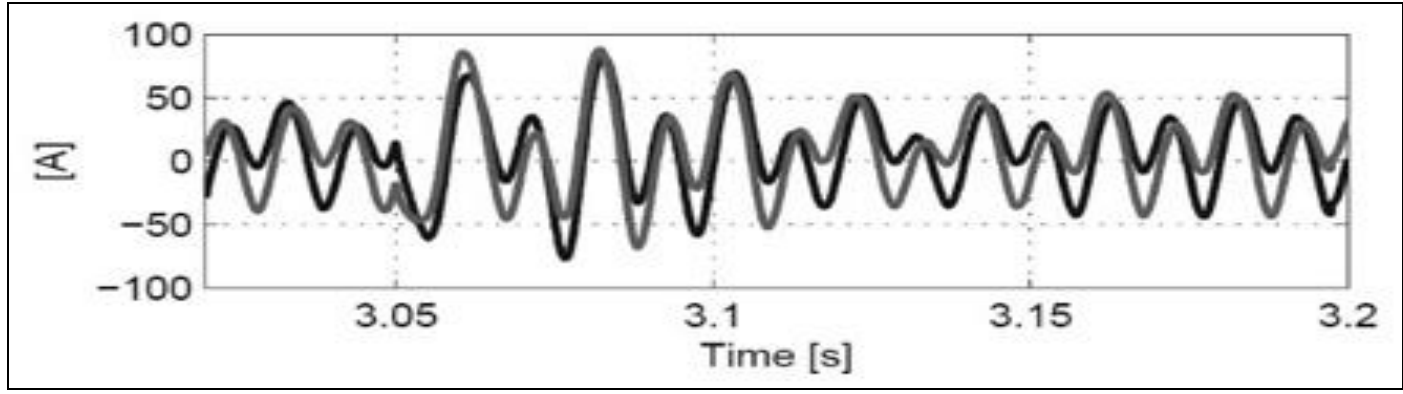


Fig 13 MC Branch Current

V. CONCLUSION

This work demonstrates the effectiveness of an innovative approach combining multilevel converters with model predictive control. Simulation results confirm system performance: generation of six voltage levels with capacitor balancing, and robustness against sudden DC voltage variations. The developed average-value model faithfully reproduces the behavior of the three-phase MC while reducing computational load, while the multi-objective cost function globally optimizes current tracking, circulating current reduction, and capacitor balancing.

REFERENCES

- [1]. M. G. a. R. Marquardt, «A New AC/AC Multilevel Converter Family,» IEEE Trans. Ind. Electron., vol. 52, n° %13, pp. 662-669, Jun. 2005.
- [2]. B. W. R. L. F. M. P. a. N. R. Z. A. Dekka, «Evolution of Topologies, Modeling, Control Schemes, and Applications of Modular Multilevel Converters,» IEEE J. Emerg. Sel. Top. Power Electron, doi: 10.1109/JESTPE.2017.2742938, vol. 5, n° %14, p. 1631–1656, Dec. 2017.
- [3]. J. A. Ferreira, «The Multilevel Modular DC Converter,» IEEE Trans. Power Electron.,doi: 10.1109/TPEL.2012.2237413, vol. 28, n° %110, p. 4460–4465, Oct. 2013.
- [4]. E. F. C. a. C. Bordons, Model predictive control, London, New York: Springer, 2004.
- [5]. A. L. a. M. L. R. Kennel, «Generalized predictive control (GPC)-ready for use in drive applications?,» IEEE 32nd Annual Power Electronics Specialists Conference, vol. 4, p. 1839–1844, Jun. 2001.
- [6]. S. Mariethoz and M. Morari, «Explicit Model-Predictive Control of a PWM Inverter With an LCL filter,» IEEE Trans. Ind. Electron., vol. 56, n° %12, p. 389–399, Feb. 2009.
- [7]. B. Z. Y. W. G. Li, «A modified modular multilevel converter with reduced capacitor voltage fluctuation",» EEE Trans. Ind. Electron., p. 6108–6119, 2015.
- [8]. K. L. Y. Z. Z. Wang, «Voltage balancing and fluctuation-suppression methods of floating capacitors in a new modular multilevel converter,»

IEEE Trans. Ind. Electron.,, vol. 60, n° %15, p. 1943–1954, 2013.